*Anal. Chem.* **2007,** *79,* 7883−7892

# MS/MS Simplification by 355 nm Ultraviolet Photodissociation of Chromophore-Derivatized Peptides in a Quadrupole Ion Trap

**Jeffrey J. Wilson and Jennifer S. Brodbelt***

*Department of Chemistry and Biochemistry, University of Texas at Austin, 1 University Station A5300, Austin, Texas 78712*

**Ultraviolet photodissociation (UVPD) of chromophore-modified peptides enhances the capabilities for de novo sequencing in a quadrupole ion trap mass spectrometer. Attachment of UV chromophores allows efficient photoactivation of not only the precursor ions but also any fragments that retain the chromophore functionality. For doubly protonated peptides, UVPD leads to a vast reduction in MS/MS complexity. The array of b and y ions typically seen upon collisionally activated dissociation is reduced to a single series of either y or b ions by UVPD depending on the location of the chromophore (i.e., N- or C-terminus). The sulfonation reagent Alexa Fluor 350 (AF350) provided the best overall results for the singly and doubly charged peptides by UVPD. The nonsulfonated analogue of AF350, 7-amino-4-methylcoumarin-3-acetic acid, also led to simplified spectra for doubly charged, but not singly charged, peptides by UVPD. Dinitrophenyl-peptides also yielded simplified spectra by UVPD albeit with a small amount of internal fragments accompanying the series of diagnostic y ions. The success of this MS/MS simplification process stems from extensive secondary fragmentation of any chromophore-containing fragments upon exposure to subsequent laser pulses. Energy-variable UVPD reveals that the abundances of non-chromophore-containing y fragment ions increase linearly with laser pulse energy, suggesting secondary dissociation of these species is insignificant. The abundances of chromophore-containing a/b fragment ions follow a quadratic trend due to the extensive secondary fragmentation at higher laser energies or multiple pulses.**

Proteomics has relied increasingly on an array of advanced mass spectrometry techniques as vital tools for characterizing biological molecules.[1,2] The advent of electrospray ionization (ESI)[3] and matrix-assisted laser desorption/ionization (MALDI),[4,5] especially when coupled with tandem mass spectrometry, has been at the forefront of this success.[6−8] A variety of tandem mass spectrometry techniques has been developed for peptide sequencing, including collisional activated dissociation (CAD),[9,10] infrared multiphoton dissociation (IRMPD),[11−13] electron capture dissociation (ECD),[14] electron-transfer dissociation (ETD),[15−17] ultraviolet photodissociation (UVPD),[18−21] surface-induced dissociation,[22] and postsource decay.[23] CAD, being the most popular method to date, facilitates low-energy fragmentation pathways primarily creating y and b ions by means of cleavage at the amide bond along the peptide backbone. More recently ECD in FTICR instruments[14] and ETD in linear ion trap instruments,[15−17] where c and z peptide fragment ions dominate, offer complementary MS/MS information compared to conventional CAD methods and are particularly promising for the elucidation of posttranslational modifications.

MS/MS spectra of peptides from protein digests typically contain massive amounts of information, which are often cumbersome if not impossible to manually interpret in an efficient manner, especially for more complex samples such as those containing new proteomes where primary sequence information is not readily available. This problem is exacerbated by dissociation methods

* To whom correspondence should be addressed. E-mail: jbrodbelt@mail.utexas.edu.

(1) Winston, R.; Fitzgerald, M. *Mass Spectrom. Rev.* **1997**, *16*, 165−179.
(2) Godovac-Zimmermann, J.; Brown, L. *Mass Spectrom. Rev.* **2001**, *20*, 1−57.
(3) Fenn, J.; Mann, M.; Meng, C.; Wong, S.; Whitehouse, C. *Science* **1989**, *246*, 64−71.
(4) Tanaka, K. W.; Hiroaki, I.; Yutaka, A.; Satoshi, Y.; Yoshikazu, Y. T. *Rapid Commun. Mass Spectrom.* **1988**, *2*, 151−153.
(5) Karas, M.; Hillenkamp, F. *Anal. Chem.* **1988**, *60*, 2299−2301.
(6) Regnier, F.; Riggs, L.; Zhang, R.; Xiong, L.; Liu, P.; Chakraborty, A.; Seeley, E.; Sioma, C.; Thompson, R. *J. Mass Spectrom.* **2002**, *37*, 133−145.
(7) Lill, J. *Mass Spectrom. Rev.* **2003**, *22*, 182−194.
(8) Wysocki, V.; Resing, K.; Zhang, Q.; Cheng, G. *Methods* **2005**, *35*, 211−222.
(9) Wells, J.; McLuckey, S. *Methods Enzymol.* **2005**, *402*, 148−185.
(10) Laskin, J.; Futrell, J. *Mass Spectrom. Rev.* **2003**, *22*, 158−181.
(11) Little, D.; Speir, J.; Senko, M.; OConnor, P.; McLafferty, F. *Anal. Chem.* **1994**, *66*, 2809−2815.
(12) Crowe, M.; Brodbelt, J. *J. Am. Soc. Mass Spectrom.* **2004**, *15*, 1581−1592.
(13) Payne, A.; Glish, G. *Anal. Chem.* **2001**, *73*, 3542−3548.
(14) Zubarev, R. *Curr. Opin. Biotechnol.* **2004**, *15*, 12−16.
(15) Syka, J.; Coon, J.; Schroeder, M.; Shabanowitz, J.; Hunt, D. *Proc. Natl. Acad. Sci. U.S.A.* **2004**, *101*, 9528−9533.
(16) Coon, J.; Shabanowitz, J.; Hunt, D.; Syka, J. *J. Am. Soc. Mass Spectrom.* **2005**, *16*, 880−882.
(17) Coon, J.; Ueberheide, B.; Syka, J.; Dryhurst, D.; Ausio, J.; Shabanowitz, J.; Hunt, D. *Proc. Natl. Acad. Sci. U.S.A.* **2005**, *102*, 9463−9468.
(18) Choi, K.; Yoon, S.; Sun, M.; Oh, J.; Moon, J.; Kim, M. *J. Am. Soc. Mass Spectrom.* **2006**, *17*, 1643−1653.
(19) Thompson, M.; Cui, W.; Reilly, J. *Angew. Chem., Int. Ed.* **2004**, *43*, 4791−4794.
(20) Oh, J.; Moon, J.; Kim, M. *Rapid Commun. Mass Spectrom.* **2004**, *18*, 2706−2712.
(21) Gabryelski, W.; Li, L. *Rev. Sci. Instrum.* **1999**, *70*, 4192−4199.
(22) Dongre, A.; Somogyi, A.; Wysocki, V. *J. Mass Spectrom.* **1996**, *31*, 339−350.
(23) Chaurand, P.; Luetzenkirchen, F.; Spengler, B. *J. Am. Soc. Mass Spectrom.* **1999**, *10*, 91−103.

10.1021/ac071241t CCC: $37.00 
Published on Web 09/11/2007

that characteristically induce backbone cleavage and yield a large number of fragment ions providing redundant sequence information, thus cluttering the MS/MS spectra and hampering peptide identification even with the use of elegant spectral interpretation and database search algorithms. These issues have fueled efforts to develop more selective fragmentation patterns via new activation methods or via peptide derivatization strategies to simplify the resulting MS/MS data.[24−37] For example, Keough et al. reported an N-terminal sulfonation derivatization strategy for peptides that resulted in the formation of a series of y ions absent of redundant b ion fragments upon postsource decay of singly protonated peptides in a MALDI time-of-flight (TOF) instrument.[24] Because of the incorporation of a negatively charged sulfonate group at the N-terminus, any b-type fragments formed are zwitterionic and thus not detected, leaving a distinct series of diagnostic singly charged y ions. This technique has become quite successful for de novo interpretation applications in MALDI-TOF instruments[24−32] and also has shown promise in ESI-quadrupole ion trap (QIT) instruments.[33−37] The success of this N-terminal sulfonation derivatization method with respect to simplifying tandem mass spectra of peptides depends on the formation and analysis of singly charged peptide ions because multiply charged peptides produce both b and y ions upon dissociation. Other groups have refined the N-terminal sulfonation protocol or revised the sulfonation reagents to further improve the efficiency of the derivatization method and its general applicability for de novo sequencing.[36−44] For example, Lee et al. has demonstrated the utility of an isotope-coded sulfonation reagent for analysis of doubly charged peptides in which the b ions are easily recognized because they appear as doublet peaks separated by 6 Da due to the differential mass labeling of the N-terminus.[36] Our group has recently implemented IRMPD for sequencing of N-terminally sulfonated tryptic peptides to create a complete series of y ions down to the $y_1$ fragment for enhanced MS/MS characterization in a QIT.[37] Other derivatization strategies also have been developed for peptides to assist in sequencing applications. For example, an N-terminal phosphonylation procedure has been reported that promotes the formation of b ions, rather than y ions, upon CAD.[38,39] Reilly's group has developed an N-terminal amidination procedure that enhances the formation of $y_{n-1}$ ions and thus is useful for constraining database searches.[40,41] Another procedure entails the formation of N-terminal phenylthiocarbamoyl derivatives that yield $b_1$ ions upon dissociation, thus allowing confident identification of the N-terminal residues of peptides.[42,43] More recently Yamaguchi et al. reported a C-terminal derivatization procedure via imidazoline chemistry that allowed convenient C-terminal sequencing of proteins.[44] We extend this theme of selective modification of peptides in the present study by combining N-terminal derivatization in conjunction with UV photodissociation for de novo sequencing.

In the ongoing search for more universal activation methods, photodissociation has generated considerable interest.[18−21,45−56] Photodissociation offers particular advantages for quadupole ion traps, including the nonresonant nature of activation and the independence of the photoactivation process on the rf trapping voltage, which allows use of a low rf trapping voltage and storage of low $m/z$ fragment ions. Retention of the low $m/z$ range is important for sequencing the last few C-terminal and N-terminal residues of peptides. While IRMPD has been promising for several recent applications involving quadrupole ion traps,[12,13,37] energy deposition is limited due to the low energy per photon (~0.1 eV at 10.6 $\mu$m) and substantial competition from collisional deactivation that occurs with 1 mTorr helium in the trap. UVPD, the activation method featured in the present study, offers the advantage of substantially higher energy deposition per photon (e.g., 3.5 eV at 355 nm), in addition to incorporating a degree of selectivity into the dissociation strategy based on addition of UV chromophores to analytes of interest.

There has been a recent surge of interest in UVPD, in part because of its natural compatibility with time-of-flight, quadrupole ion trap, and linear ion trap instruments.[18−21,45−56] UVPD has shown great potential as a viable fragmentation method for unmodified


(24) Keough, T.; Youngquist, R.; Lacey, M. *Proc. Natl. Acad. Sci. U.S.A.* **1999**, *96*, 7131−7136.
(25) Keough, T.; Lacey, M.; Youngquist, R. *Rapid Commun. Mass Spectrom.* **2000**, *14*, 2348−2356.
(26) Wang, D.; Kalb, S.; Cotter, R. *Rapid Commun. Mass Spectrom.* **2004**, *18*, 96−102.
(27) Samyn, B.; Debyser, G.; Sergeant, K.; Devreese, B.; Van, Beeumen, J. *J. Am. Soc. Mass Spectrom.* **2004**, *15*, 1838−1852.
(28) Wang, D.; Cotter, R. *Anal. Chem.* **2005**, *77*, 1458−1466.
(29) Wang, D.; Xu, W.; McGrath, S.; Patterson, C.; Neckers, L.; Cotter, R. *J. Proteome Res.* **2005**, *4*, 1554−1560.
(30) Pashkova, A.; Chen, H.; Rejtar, T.; Zang, X.; Giese, R.; Andreev, V.; Moskovets, E.; Karger, B. *Anal. Chem.* **2005**, *77*, 2085−2096.
(31) Oehlers, L.; Perez, A.; Walter, R. *Rapid Commun. Mass Spectrom.* **2005**, *19*, 752−758.
(32) Guillaume, E.; Panchaud, A.; Affolter, M.; Desvergnesand, V.; Kussmann, M. *Proteomics* **2006**, *6*, 2338−2349.
(33) Bauer, M.; Sun, Y.; Keough, T.; Lacey, M. *Rapid Commun. Mass Spectrom.* **2000**, *14*, 924−929.
(34) Lee, Y.; Kim, M.; Choie, W.; Min, H.; Lee, S. *Proteomics* **2004**, *4*, 1684−1694.
(35) Wang, D.; Kalume, D.; Pickart, C.; Pandey, A.; Cotter, R. *Anal. Chem.* **2006**, *78*, 3681−3687.
(36) Lee, Y.; Han, H.; Chang, S.; Lee, S. *Rapid Commun. Mass Spectrom.* **2004**, *18*, 3019−3027.
(37) Wilson, J.; Brodbelt, J. *Anal. Chem.* **2006**, *78*, 6855−6862.
(38) Bao, J.; Ai, H.; Fu, H.; Jiang, Y.; Zhao, Y.; Huang, C. *J. Mass Spectrom.* **2005**, *40*, 772−776.
(39) Wang, F.; Fu, H.; Jiang, Y.; Zhao, Y. *J. Am. Soc. Mass Spectrom.* **2006**, *17*, 995−999.
(40) Beardsley, R.; Reilly, J. *J. Am. Soc. Mass Spectrom.* **2004**, *15*, 158−167.
(41) Beardsley, R.; Sharon, L.; Reilly, J. *Anal. Chem.* **2005**, *77*, 6300−6309.
(42) Brancia, F.; Butt, A.; Beynon, R.; Hubbard, S.; Gaskell, S.; Oliver, S. *Electrophoresis* **2001**, *22*, 552−559.
(43) Summerfield, S.; Bolgar, M.; Gaskell, S. *J. Mass Spectrom.* **1997**, *32*, 225−231.
(44) Yamaguchi, M.; Oka, M.; Nishida, K.; Ishida, M.; Hamazaki, A.; Kuyama, H.; Ando, E.; Okamura, T.; Ueyama, N.; Norioka, S.; Nishimura, O.; Tsunasawa, S.; Nakazawa, T. *Anal. Chem.* **2006**, *78*, 7861−7869.
(45) Hettick, J.; McCurdy, D.; Barbacci, D.; Russell, D. *Anal. Chem.* **2001**, *73*, 5378−5386.
(46) Barbacci, D.; Russell, D. *J. Am. Soc. Mass Spectrom.* **1999**, *10*, 1038−1040.
(47) Guan, Z.; Kelleher, N.; O'Connor, P.; Aaserud, D.; Little, D.; McLafferty, F. *Int. J. Mass Spectrom. Ion Processes* **1996**, *158*, 357−364.
(48) Moon, J.; Yoon, S.; Kim, M. *Rapid Commun. Mass Spectrom.* **2005**, *19*, 3248−3252.
(49) Morgan, J.; Russell, D. *J. Am. Soc. Mass Spectrom.* **2006**, *17*, 721−729.
(50) Williams, E.; Furlong, J.; McLafferty, F. *J. Am. Soc. Mass Spectrom.* **1990**, *1*, 288−294.
(51) Fung, Y.; Kjeldsen, F.; Silivra, O.; Chan, T.; Zubarev, R. *Angew. Chem., Int. Ed.* **2005**, *44*, 6399−6403.
(52) Kjeldsen, F.; Silivra, O.; Zubarev, R. *Chem. Eur. J.* **2006**, *12*, 7920−7928.
(53) Kim, T.; Thompson, M.; Reilly, J. *Rapid Commun. Mass Spectrom.* **2005**, *19*, 1657−1665.
(54) Zhang, L.; Cui, W.; Thompson, M.; Reilly, J. *J. Am. Soc. Mass Spectrom.* **2006**, *17*, 1315−1321.
(55) Oh, J.; Moon, J.; Kim, M. *J. Mass Spectrom.* **2005**, *40*, 899−907.
(56) Oh, J.; Moon, J.; Lee, Y.; Hyung, S.; Lee, S.; Kim, M. *Rapid Commun. Mass Spectrom.* **2005**, *19*, 1283−1288.

peptides[18−20,46−55] and offers the ability to tune energy deposition based on the specific laser wavelength and photon flux. Several types of lasers have been utilized for UVPD, including excimer (ArF at 193 nm; 6.2 eV,[18,45−50] and $F_2$ at 157 nm; 7.9 eV),[19,51−54] and Nd:YAG (fourth harmonic at 266 nm, 4.7 eV)[20,21,55,56] lasers. The excimer lasers provide sufficiently high photon energies that absorption of a single photon can promote backbone and side chain cleavage to produce a, d, x, v, and w fragment ions.[18,19,48,49,52−54] Zubarev et al. demonstrated that 157 nm UVPD preferentially cleaves disulfide bonds in peptide structures, thus facilitating de novo sequencing for peptides containing this functionality.[51] In addition, Zubarev's group was able to exploit 157 nm UVPD for probing the zwitterionic states of peptides in the gas phase.[52] Photodissociation at 266 nm mimics lower energy activation methods in which the majority of the MS/MS spectra are composed of b and y fragment ions.[20,21,55,56]

Despite the promise of UVPD for characterization of biological molecules, this strategy requires that the ions of interest absorb at the wavelength of the laser. Many peptides do not have appropriate chromophores that overlap with common laser wavelengths, and this has limited the general applicability of UVPD. To date only Russell et al. have explored peptide modifications for the enhancement of UVPD efficiency.[57,58] The first study used a cw argon ion laser for dissociation of dinitrophenyl-modified dipeptides in a EB/E sector instrument.[57] The second study reported characterization of a dinitrophenyl-modified hexapeptide by 337 nm excitation from a pulsed $N_2$ laser;[58] however, this method was not extended to larger peptides due to low fragmentation efficiencies achieved by this low-energy $N_2$ laser.

In this study, we demonstrate the application of UVPD in a quadrupole ion trap mass spectrometer to improve de novo sequencing of chromophore-modified peptides. Whereas an array of a/b and y ions is created by traditional CAD of doubly charged, dinitrophenyl, 7-amino-4-methyl coumarin-3-acetic acid, or Alexa Fluor 350 N-terminally derivatized peptides, UVPD at 355 nm (3.5 eV per photon) results in spectra dominated by y ions because the redundant chromophore-containing a/b ions are eliminated by secondary UVPD. In contrast, for C-terminally modified peptides, abundant a/b type ions are the major fragment ions observed upon UVPD due to the rapid elimination of the chromophore-containing y ions.

## EXPERIMENTAL SECTION

**Reagents.** All chemicals were purchased from Sigma Aldrich (St. Louis, MO) except the following: Alexa Fluor 350 carboxylic acid, succinimidyl ester (AF350) from Invitrogen (Carlsbad, CA); 6-(2,4-dinitrophenyl)aminohexanoic acid, succinimidyl ester (DNP) from Anaspec (San Jose, CA), and 7-amino-4-methylcoumarin-3-acetic acid, succinimidyl ester (AMCA) from Pierce Biotechnology (Rockford, IL). All peptides were purchased from Bachem (King of Prussia, PA) except fibrinopeptide A (ADSGEGDFLAEGGGVR), which was obtained from American Peptide Co. (Sunnyvale, CA).

**Mass Spectrometry.** A ThermoFinnigan LCQ Deca XP (San Jose, CA) modified with both IRMPD and UVPD capabilities was utilized for all mass spectrometry experiments as described in more detail below. Solutions were prepared at a concentration of 10 $\mu$M in a 50/50/1 MeOH/$H_2O$/HOAc (v/v) solvent mixture for ESI-MS analysis. These solutions were infused into the mass spectrometer at a flow rate of 3 $\mu$L/min with a Harvard Apparatus PHD 2000 syringe pump (Holliston, MA). Ion activation by CAD was conducted at the default $q_z$ value of 0.25 for 30 ms. Energy-variable CAD experiments were collected in triplicate, and the standard deviations of the CAD activation voltages, defined as the CAD voltage at which 50% of the abundance of the precursor ion survives, are less than 0.01 V.

**Infrared Multiphoton Dissociation.** IRMPD experiments were carried out on an LCQ Deca XP instrument equipped with a 48-5 Synrad 50-W $CO_2$ continuous wave laser (Mukilteo, WA), which has been previously described in full detail.[37] In brief, the laser beam was aligned through a ZnSe window mounted on a CF viewport flange and a 5-mm hole drilled in the ring electrode for photoactivation of the ion cloud. The laser was triggered during the activation segment of the scan function for photodissociation with a low $q_z$ value of typically 0.10 to provide a considerable reduction in the low mass cutoff compared to conventional CAD in which $q_z = 0.25$.

**Ultraviolet Photodissociation.** UVPD was also performed on this LCQ Deca XP instrument equipped with a Quanta-Ray GCR-11 Nd:YAG laser with a HG-2 harmonics generator from Spectra-Physics (Mountain View, CA) for creation of the tripled harmonic photons at 355 nm. The CF viewport flange on the vacuum manifold permitted switching the window to an antireflective quartz window from CVI laser (Albuquerque, NM) for transmission of the UV photons. The laser beam was used without focusing or collimation. The Nd:YAG laser was gated at the appropriate point in the scan function using a TTL signal output from the mass spectrometer at pin TP 15-3_Sync_TP and controlled by the LCQ software. This instrument TTL signal was fed into an operational amplifier circuit integrated into the laser control unit set to increase the instrument TTL signal to the necessary 15 V for triggering the laser. The laser was typically operated at 10 Hz and with full energy (~60 mJ/ pulse) in the Q-switched mode with the number of pulses reported. At 15 Hz, each pulse was ~20 mJ/pulse when compared to the 10-Hz mode of operation. For energy-variable experiments, a beam splitter was used to sample a small fraction of the laser beam during UVPD experiments and monitored with an UV detection element (PD300-UV-SH) coupled to an Ophir Optronics laser power meter AN/2 (Wilmington, MA) to determine the relative energy in relation to the 60 mJ/pulse at full power.

**Ion Trap Helium Pressure.** The LCQ ion trap instrument was also modified with a Porter flow control device, VCD-1000, with a 5 $cm^3$/min max flow element (Hatfield, PA), which was installed in-line with the helium gas flow to the ion trap for helium pressure control. This flow valve was utilized for measuring the extent of dissociation versus relative changes in helium pressure within the ion trap. The optimal buffer gas pressure, as defined by maximum trapping efficiency, corresponded to a nominal chamber pressure of $3.0 \times 10^{-5}$ Torr with the ZnSe window and $2.8 \times 10^{-5}$ Torr with the quartz window, each of which is equivalent to ~1 mTorr of helium in the trapping region. The optimal ion trap helium pressures were used for all experiments shown except for the helium variable experiments.

(57) Tecklenburg, R.; Miller, M.; Russell, D. *J. Am. Chem. Soc.* **1989**, *111*, 1161−1171.
(58) Solouki, T.; Russell, D. *Appl. Spectrosc.* **1993**, *47*, 211−217.

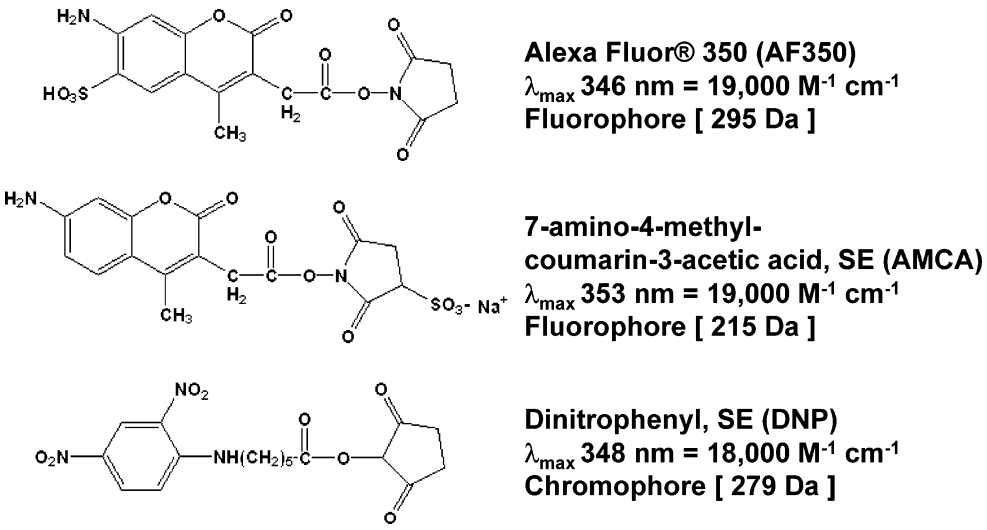


**Figure 1.** Chemical structures of the *N*-hydroxysuccinimidyl ester (SE) derivatization agents used for N-terminal modification and the chemical abbreviation. The solution-phase molar absorptivity at the $\lambda_{max}$ is given,[61] as well as the category of the reagent and the nominal mass addition to a peptide in brackets.

**Peptide Derivatization.** The reactions for all the derivatization procedures are based on the well-established *N*-hydroxysuccinimidyl ester chemistry. In short, the reagent (AF350, AMCA, or DNP) was dissolved in extra dry DMSO at ~35 mM. This solution was then immediately added to a sodium bicarbonate buffered peptide solution, nominally at pH 8.5, at a 20:1 molar ratio. The reaction mixture was vortexed for 30 s and then incubated at room temperature for 10 min. Individual peptides were desalted and removed from excess reagent by PepClean $C_{18}$ spin columns from Pierce Biotechnology (Rockford, IL) and then diluted for subsequent ESI-MS analysis. Although ESI suppression effects and in-source dissociation of the derivatized peptides can skew the determination of reaction yields based upon mass spectral data, the derivatization efficiencies were estimated as ~30−60% for DNP reactions and >75% for both AMCA and AF350 reactions based on comparison of the ion abundances of the derivatized peptides to those of unmodified peptides.

## RESULTS AND DISCUSSION

Comparison of the CAD and UVPD dissociation methods for derivatized peptides in a quadrupole ion trap was undertaken in order to assess the diagnostic quality of the MS/MS spectra for de novo interpretation. Additionally, the performance advantages and limitations of UVPD in comparison to traditional CAD for activation of these modified peptides were also systematically explored. Peptides do not contain natural chromophores at 355 nm; therefore, highly chromophoric functional groups were added to the peptides prior to UVPD. Figure 1 shows three derivatization reagents used in the present study: AF350, AMCA, and DNP. These three reagents react with primary amines such as those found at the N-terminus and $\epsilon$-amine of lysine side chains on peptides via conventional *N*-hydroxysuccinimidyl ester coupling chemistry.

**Enhanced MS/MS Spectra of Derivatized Peptides by Ultraviolet Photodissociation.** MS/MS spectra obtained for peptides either are often overly complex due to redundant fragment ions (i.e., a combination of a, b, and y ions) or in other cases provide limited fragment information due to lack of a mobile proton. Either situation hinders de novo interpretation, especially if the primary protein sequence is unknown. For example, singly protonated FSWGAEGQR lacks a mobile proton and consequently undergoes limited backbone fragmentation upon collisional activation.[59] The acidic side chain group of the glutamic acid at position 6 induces cleavage at its C-terminal amide bond, resulting in the abundant $y_3$ ion relative to other pathways (Figure 2A). Other fragment ions are also present in low abundance with a variety of b and y ions, including secondary losses of water and internal fragments, yielding a high degree of MS/MS spectral complexity. Derivatization of FSWGAEGQR via AF350, an N-terminal sulfonation reagent, results in formation of singly charged peptides that

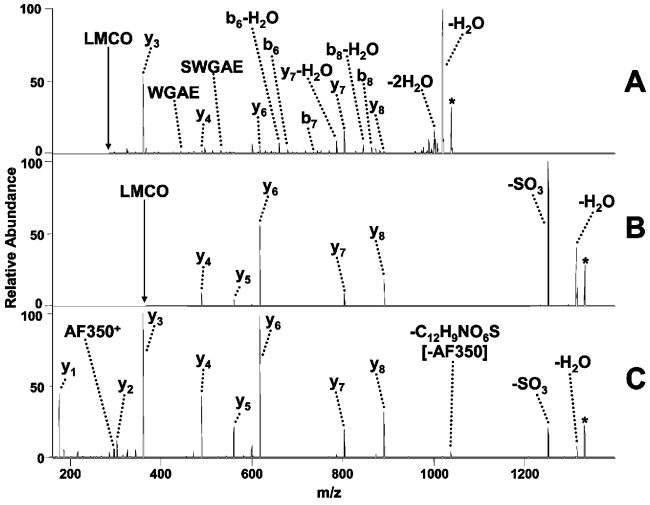


**Figure 2.** ESI-MS/MS spectra of singly protonated FSWGAEGQR (A) CAD (1.54 V) of the unmodified peptide, (B) CAD (1.31 V) of the AF350-derivatized peptide, and (C) UVPD (10 pulses at 10 Hz) of the AF350-derivatized peptide. The peak with the $C_{12}H_9NO_6S$ label corresponds to the loss of the charged AF350 moiety from the N-terminus of the peptide, thus producing the unmodified, singly charged peptide species. An asterisk (*) is used to signify the precursor ion.

(59) Wysocki, V.; Tsaprailis, G.; Smith, L.; Breci, L. *J. Mass Spectrom.* **2000**, *35*, 1399−1406.

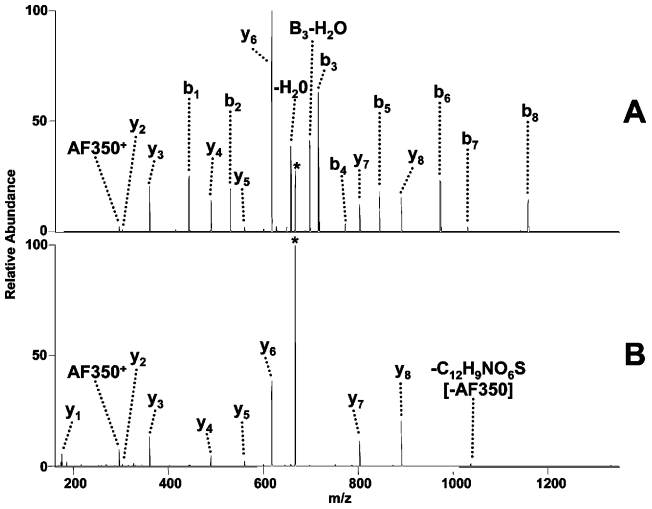


**Figure 3.** ESI-MS/MS spectra of doubly protonated N-terminally modified AF350-FSWGAEGQR peptide by (A) CAD (0.50 V) and (B) UVPD (15 pulses at 10 Hz). UVPD shows a complete series of y ions with minimal complexity due to elimination of the redundant b ions. The peak with the $C_{12}H_9NO_6S$ label corresponds to the loss of the charged AF350 moiety from the N-terminus of the peptide, thus producing the unmodified, singly charged peptide species. An asterisk (*) is used to signify the precursor ion.

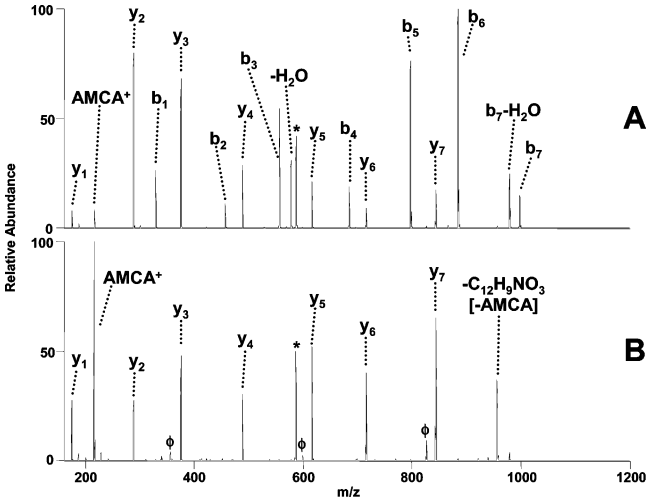


**Figure 4.** ESI-MS/MS spectra of doubly protonated N-terminally modified AMCA-LQVQLSIR peptide by (A) CAD (0.64 V) and (B) UVPD (10 pulses at 15 Hz; ~10 mJ/pulse). UVPD shows a complete series of y ions with minimal complexity due to elimination of the redundant b ion ions. The $\phi$ symbol indicates ammonia losses from the adjacent y ions. The peak with the $C_{12}H_9NO_3$ label corresponds to the loss of the charged AMCA moiety from the N-terminus of the peptide, thus producing the unmodified, singly charged peptide species. An asterisk (*) is used to signify the precursor ion.

produce a greater series of y ions upon CAD, as shown in Figure 2B. UVPD of the AF350-modified peptide yields a complete series of y ions down to the $y_1$ ion, facilitating the confident sequencing of this peptide as shown in Figure 2C. Moreover, the uninformative losses of $H_2O$ and $SO_3$ are greatly reduced upon UVPD. For singly protonated peptides modified with AMCA or DNP, the observed dissociation pathways are relatively unaffected by the derivatization reagent and thus are similar to those of their respective unmodified singly protonated peptides (see Supporting Information Figure S-1).

The generation of a complete series of y ions was also possible for singly charged N-terminally sulfonated peptides by IRMPD in an ion trap in an earlier report from our group.[37] The success of the N-terminal sulfonation derivatization strategy for de novo sequencing of peptides largely depends on the presence of a proton sequestering C-terminal basic site and the ability to produce singly protonated peptides. In fact, doubly protonated N-terminal sulfonated peptides do not yield a clean series of y ions by CAD or IRMPD; instead, both y and a/b type ions are generated, which complicates spectral interpretation. For example, Figure 3A illustrates the CAD spectrum for the doubly protonated AF350-derivatized FSWGAEGQR peptide, and the extensive array of y and b ions clutter the spectrum. Interestingly, peptide fragmentation highly disfavors formation of the $b_1$ ion; however, it is observed in Figure 3A due to the modification at the N-terminus.[42,43] In contrast, the UVPD spectrum of the same peptide shows only a series of y ions down to the $y_1$ ion (Figure 3B). The b ions, all which retain the AF350 chromophore at their N-terminus, undergo extremely efficient secondary UVPD and thus are removed from the spectrum. The y ions, none of which contain the AF350 group and thus lack the UV chromophore, do not undergo secondary UVPD. Further exploration of this prominent secondary dissociation of the chromophore-containing fragment ions is addressed in a later section within this study.

Analogous behavior is observed for peptides containing other chromophores, such as AMCA and DNP, when UVPD is employed instead of CAD. Figure 4A shows a rather complex CAD spectrum for doubly protonated AMCA-modified LQVQLSIR with a full series of both b and y ions. UVPD results in a series of y ions down to the $y_1$ ion (Figure 4B). Additionally, the abundant ion due to the loss of water observed in the CAD spectrum is not seen in the UVPD spectrum due to its efficient UV absorption and rapid dissociation into other diagnostic sequence ions. Unlike the AF350-derivatized peptide (described in the previous paragraph with representative data shown in Figure 3), the AMCA-modified peptide also undergoes some ammonia losses from the y ion series (these ammonia loss ions are labeled with a phi symbol ($\phi$) in Figure 4B). We speculate that these ammonia losses, which were not observed for the analogous AF350-derivatized peptide, could be due to the specific nature of the AMCA chromophore and the subsequent distribution of energy within the photoenergized peptide.

To evaluate whether addition of the three different chromophore functionalities (AMCA, AF350, DNP) results in any significant differences in the dissociation energies of the peptides or the relative UVPD efficiencies, one peptide (FSWGAEGQR) was derivatized and subjected to successive CAD and UVPD comparisons. First energy-variable CAD experiments in which the applied CAD activation voltage needed to induce dissociation of 50% of the precursor ion population were undertaken for AMCA-FSWGAEGQR, AF350-FSWGAEGQR, and DNP-FSWGAEGQR. The normalized CAD activation voltages (corrected for degrees of freedom) were found as follows: AMCA-FSWGAEGQR (0.94 V), DNP-FSWGAEGQR (0.96 V), and AF350-FSWGAEGQR (0.99 V). The similarity in the values suggests that the three different chromophores cause little impact on the dissociation energies of the peptides. However, when the three derivatized peptides were each subjected to UVPD using 20 laser pulses (40 mJ/pulse), the

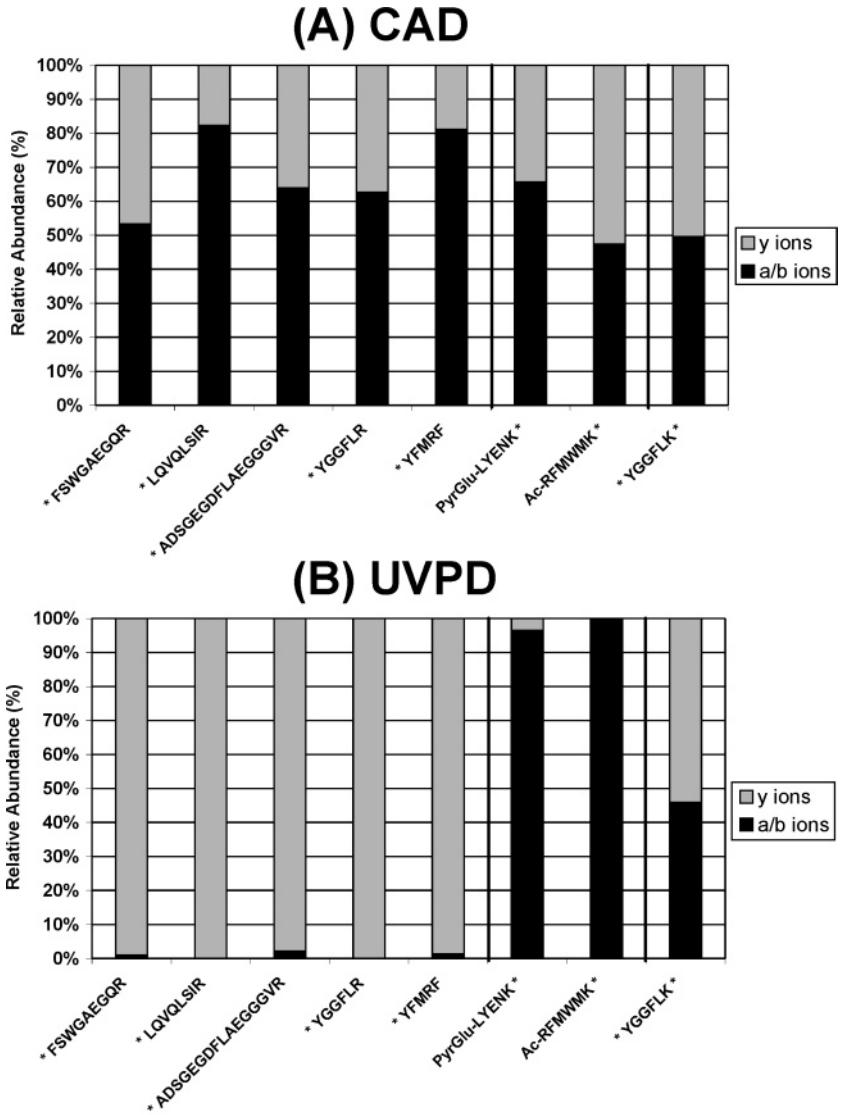


**Figure 5.** MS/MS bar graphs summarizing the summed distribution of y versus a/b ions formed upon dissociation of doubly protonated AF350-derivatized peptides. (A) CAD results and (B) UVPD results at 355 nm (10−20 pulses at 10 Hz, except for *YGGFLK* peptide collected with 10 pulses at 15 Hz; 20 mJ/pulse). The peptide sequences are shown along the *x*-axis with an asterisk (*) designating the derivatization site.

dissociation efficiency as reflected by the percentage conversion of precursor peptide ions into fragment ions varied dramatically as follows: AMCA-FSWGAEGQR (77%) > DNP-FSWGAEGQR (37%) > AF350-FSWGAEGQR (15%). We speculate that the differences in the gas-phase absorption maximums of the AF350-, AMCA-, and DNP-derivatized peptides, along with their relative abilities to undergo radiative emission, account for the observed differences in the UVPD efficiencies of these derivatized peptides. AF350 ions have previously been shown to retain their fluorogenic properties in the gas phase based on laser-induced fluorescence measurements in an ion trap,[60] and thus, competitive fluorescence would be expected based on the time scale of the experiment. Both AF350 and AMCA are well-known fluorophores in solution, and thus, it appears that their fluorescent properties are retained in the gas phase. In other words, the AF350- and AMCA-peptides may readily absorb UV photons but may undergo efficient fluorescence instead of dissociation. Although AMCA itself displays significant fluorescence in solution, we attribute the greater UVPD efficiencies of the AMCA-derivatized peptides compared to the DNP- and AF350-derivatized peptides to a higher absorption cross section at 355 nm as suggested by the reported $\lambda_{max}$ in solution experiments (Figure 1).[61] A detailed analysis of the competition between fluorescence and dissociation processes is beyond the scope of this initial work on the simplification of MS/MS spectra but will be explored in a future study.

The dramatic difference in fragmentation information based upon the two activation techniques (UVPD versus CAD) was explored for several other peptides to help establish the general potential of UVPD as a means of simplifying MS/MS spectra for de novo sequencing. Bar graphs summarizing the MS/MS data for doubly protonated AF350-derivatized peptides are shown in Figure 5 and for doubly protonated AMCA-derivatized peptides in Figure 6. In these bar graphs, the relative percentages of the total y fragment peak areas are summed and compared to the sum of the a/b fragment peak areas (all normalized to 100%). The

(60) Khoury, J.; Rodriguez-Cruz, S.; Parks, J. *J. Am. Soc. Mass Spectrom.* **2002**, *13*, 696−708.

(61) http://probes.invitrogen.com, accessed on May 2007.

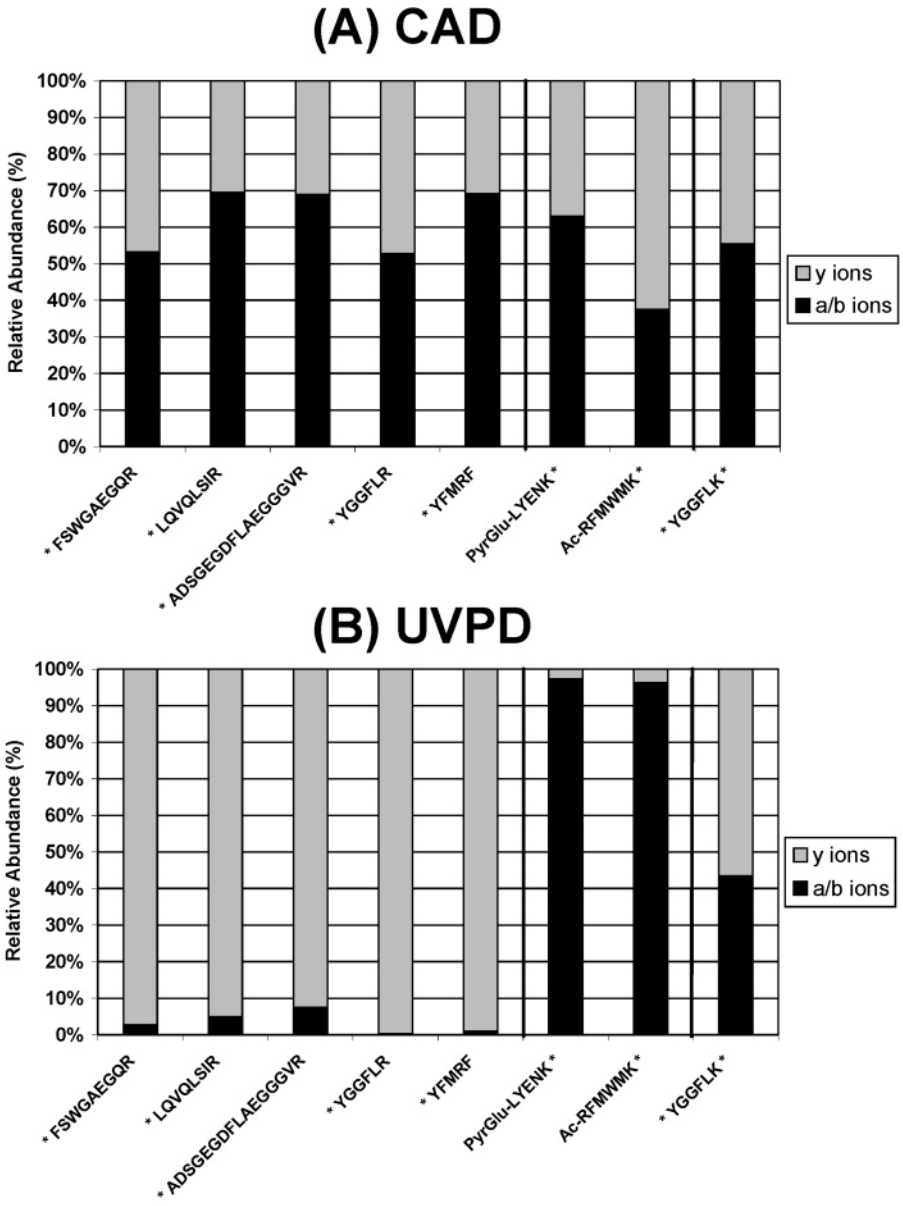


**Figure 6.** MS/MS bar graphs summarizing the summed distribution of y versus a/b ions formed upon dissociation of doubly protonated AMCA-derivatized peptides. (A) CAD results and (B) UVPD results at 355 nm (20 pulses at 15 Hz, except for *YGGFLK* peptide collected with 5 pulses at 15 Hz; 5 mJ/pulse). The peptide sequences are shown along the *x*-axis with an asterisk (*) designating the derivatization site.

peptide sequences used are shown along the *x*-axis with an asterisk denoting the location of the chromophore based on the specific modification site. The left four peptides, FSWGAEGQR, LQVQLSIR, ADSGEGDFLAEGGGVR, and YGGFLR, have a C-terminal basic site and thus mimic tryptic peptides. The addition of the chromophore occurs at the N-terminus for these four peptides. Upon UVPD, nearly exclusive formation of y ions occurs for these first four peptides, whereas CAD yields a mixture of y, b, and a ions. These four peptides all have a C-terminal arginine, but a similar strategy presumably could be used for peptides with C-terminal lysines in conjunction with guanidination of the lysines to prevent the chromophore derivatization reactions from occurring at the C-terminus. The sixth and seventh peptides, PyrGlu-LYENK and Ac-RFMWMK, both have "inverted" sequences in which the reactive amine is located at the C-terminus via the $\epsilon$-amine of lysine and the N-terminus is inaccessible to modification, meaning the UV chromophore will be located at the C-terminus after the derivatization procedure. The sixth peptide, PyrGlu-LYENK, does not have a basic N-terminal site; it produces an extensive series of a/b fragment ions as would be expected due to the location of the chromophore at the C-terminus. The seventh peptide, Ac-RFMWMK, has an N-terminal basic site to mirror inversely the first four peptides, and as expected, a complete series of a/b type fragment ions dominates the UVPD spectrum, whereas CAD produced a much more complex MS/MS spectrum containing a, b, and y ions. A complete series of a and b ions is generally less desirable than a clean series of y ions because of the redundant backbone information between a- and b-type ions. The eighth peptide, YGGFLK, was selected because it has both an accessible N-terminus and an $\epsilon$-amine lysine side chain at the C-terminus that may be modified by attachment of the AF350 chromophore. For this latter peptide, the CAD and

UVPD spectra are remarkably similar. The laser pulse energy and number of pulses were decreased to prevent complete secondary dissociation and elimination of all fragment ions from the UVPD mass spectrum of this dual-labeled peptide.

Doubly protonated AMCA-derivatized peptides were also investigated in the same manner as described above, and the CAD and UVPD results are summarized in Figure 6. The trends shown in Figure 6 for AMCA-peptides mimic those seen in Figure 5 for the analogous AF350-peptides. A complete series of y fragment ions is observed upon UVPD of each N-terminal derivatized peptide, and conversely, a complete series of a/b fragment ions is observed upon UVPD of the peptides in which the C-terminal lysine side chain is derivatized by the UV chromophore. It should be noted that whereas the AF350-modified peptides produced very clean MS/MS spectra by UVPD, the AMCA derivatives also produced some $y_n - NH_3$ fragment ions upon UVPD, similar to what was observed in Figure 4B (see the ion peaks labeled with the phi symbols).

In general, the percentage of fragment ions formed by UVPD relative to surviving precursor ions was estimated to be greater than 70% based on the following equation: $\Sigma$ fragments/[$\Sigma$ fragments + precursor] (based on peak areas of fragments and surviving precursor after UVPD) for all chromophore-derivatized peptides except fibrinopeptide A (ADSGEGDFLAEGGGVR) for which the efficiency was only ~15−20%. We speculate that the low UVPD efficiency of the latter is related to its large size, in which case, a more focused laser beam would increase the probability of multiphoton activation and greater energy deposition.

Equivalent MS/MS data obtained for the DNP-peptides also showed trends similar to those observed for the AF350- and AMCA-modified peptides; however, whereas the AF350 and AMCA-modified peptides produced very clean MS/MS spectra by UVPD, the DNP derivatives also produced some low-abundance internal fragment ions upon UVPD (Supporting Information Figure S-1). We attribute the less informative internal fragments observed for DNP-peptides to the inherent nature of the DNP chromophore that enhances formation of internal ions, whereas AMCA and AF350 suppress internal fragments by retaining a charge on the chromophore. Although AF350-peptides exhibited the highest spectral quality by UVPD, the promising data acquired for both the AMCA- and DNP-modified peptides suggest that a wide variety of chromogenic derivatization reagents could be exploited for other UV and visible PD applications.

**Variation of Laser Pulse Energy and Number of Pulses.** As mentioned earlier, the opportunity for extensive secondary dissociation of fragments that retain the chromophore is likely the major factor that leads to the simplification of the MS/MS spectra. To further elucidate this phenomenon, UVPD experiments were conducted in order to map the relative percentage of precursor ions, y ions, and a/b ions as a function of the number of laser pulses (1−20) for a series of peptides. An example of the resulting data is shown in Figure 7 for doubly protonated DNP-derivatized LQVQLSIR. Upon exposure to a single laser pulse, the peptide produces nearly equal abundances of y and a/b ions with a distribution comparable to that obtained upon CAD. However, each subsequent laser pulse results in no significant increase in the percentage of a/b ions even as the percentage of y ions continues to grow. Beyond five pulses, the percentage of a/b ions diminishes from its maximum of ~5% to near 0% after 10 or more laser pulses. From 5 to 10 pulses, the percentage of y ions rises from 40% to more than 75%. The trends illustrated in Figure 7 offer strong evidence that the fragments that retain the chromophore (i.e., all a and b ions for N-terminal derivatized DNP-LQVQLSIR) are in fact eliminated from the MS/MS spectra by extensive secondary dissociation upon multiple laser pulses.

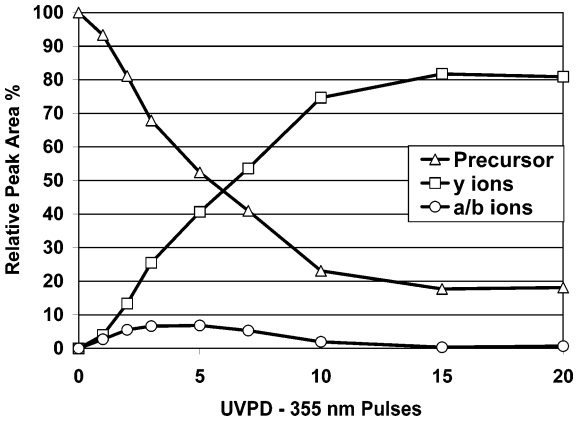


**Figure 7.** Relative peak area abundance versus the number of laser pulses (355 nm, 60 mJ/pulse at 10 Hz) of doubly protonated DNP-LQVQLSIR species.

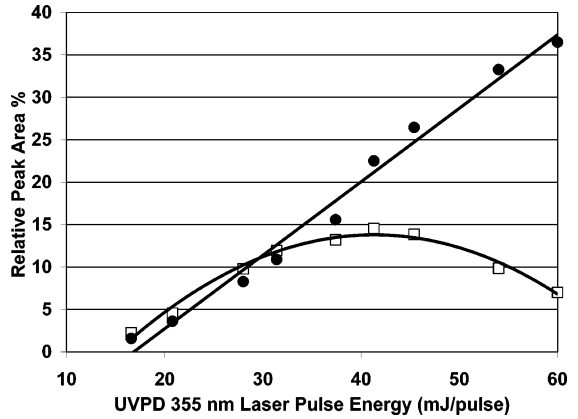


**Figure 8.** Relative peak area abundance versus the laser pulse energy (mJ/pulse) for UVPD of doubly protonated AF350-YFMRF (10 pulses at 10 Hz and 355 nm). Chromophore-containing fragments containing the AF350 moiety are denoted by the open squares (□), and the nonchromophore containing fragments are denoted by the filled circles (●). The nonchromophore fragments follow a linear trend with $R^2 = 0.985$ as a function of pulse energy, whereas the chromophore fragments follow a quadratic trend with $R^2 = 0.982$.

Energy-variable UVPD experiments were also conducted to reveal the impact of photon flux on the secondary dissociation of the chromophore-containing fragment ions. For this set of experiments, doubly protonated N-terminally derivatized AF350-YFMRF was exposed to 10 laser pulses while the laser energy per pulse was increased. Figure 8 shows the resulting energy-variable UVPD results for the summed peak areas of all chromophore-containing a/b fragment ions (□) and the summed peak areas of the non-chromophore-containing y fragment ions (●). The increase in abundance of the nonchromophore y ions follows a linear trend ($R^2 > 0.98$) with respect to laser pulse energy, showing an insignificant degree of secondary dissociation. In contrast, the abundance of the chromophore-containing a/b ions exhibits a nonlinear trend at pulse energies greater than 30 mJ/pulse,

indicating that the rate of secondary dissociation becomes more pronounced at higher pulse energies. A quadratic equation fit to the data for the chromophore-containing fragment ions yields a value of $R^2$ greater than 0.98, which implies that this trend is the product of two linear trends with the first one related to dissociation of the initial precursor ions and the second one related to secondary dissociation of the primary fragment ions. The combined pulse-variable and energy-variable data suggest that the simplification of peptide fragmentation patterns by UVPD is dependent on total photon flux, and thus, the method could likely be adapted to LC−MS applications via efficient focusing of the laser beam or use of higher repetition rate lasers (i.e., to improve the duty cycle of UVPD).

Another example illustrating the impact of secondary dissociation can be made through a more rigorous comparison of UVPD and CAD for one model peptide. For the $2^+$ AF350-YFMRF peptide, CAD (0.57 V at 30 ms), UVPD (10 pulses at 60 mJ/pulse), and isolation-only (no activation) mass spectra were collected in an alternating fashion in five replicate trials. The peak area of the isolated doubly protonated AF350-YFMRF over this period showed no significant change; thus, the average of these values was used to establish the precursor ion abundance. The portion of the precursor ions that dissociated was used to calculate the percentage of y ions and a/b ions obtained upon CAD versus UVPD. CAD produces 10.1 ± 0.3% y ions and 25.8 ± 0.6% a/b ions, with the other 65% of the ion current attributed to neutralization, scattering, fragment ions below the low mass cutoff, and surviving precursor ions. In contrast, UVPD produced 10.6 ± 0.9% y ions and only 0.1 ± 0.7% a/b ions. Based on these values, it is clear that a similar portion of the nonchromophoric y ions are formed by CAD and UVPD; however, there is a major difference in the portion of a/b ions. These values confirm that a/b-type fragment ions must be formed upon UV irradiation but dissociate to form nondetectable products in subsequent UV pulses, thus removing them from the UVPD mass spectra. What are these nondetectable products? We speculate that upon dissociation into what would normally be internal product ions from secondary dissociation of y- or b-type ions, the proton could reside on the chromophore (AF350 and AMCA) through the aniline functionality. The chromophore moiety may undergo dissociation that produces fragments of very low $m/z$ that are not detectable. In contrast, DNP does not have this aniline functionality, and the internal ions are indeed observed for peptides modified with this chromophore.

**Effect of Ion Trap Buffer Gas Pressure on Dissociation Efficiency.** The efficiency and sensitivity of many activation techniques employed in ion traps are dependent upon the helium bath gas pressure. For instance, CAD requires numerous collisions for sufficient energy accumulation prior to ion dissociation; however, high helium pressures result in collision frequencies that are too great to allow substantial acceleration of ions between collisions, resulting in low ion kinetic energies and poor energy transfer. For IRMPD experiments, high pressures lead to excessive collisional cooling that competes with energy accumulation, resulting in low dissociation efficiencies. Lower pressures enhance IRMPD efficiencies at the expense of ion trapping efficiency, ultimately resulting in lower ion signals. Conversely, UVPD provides such rapid and high-energy deposition per photon that collisional cooling does not compete substantially on the same time scale. The impact of helium pressure on the efficiencies of CAD, IRMPD, and UVPD is summarized in Figure 9 in which the dissociation efficiency of DNP-modified PQG peptide is monitored as a function of the helium pressure, as controlled by an in-line helium leak valve. The optimal pressure was nominally 30 $\mu$Torr (uncorrected) at which total ion trapping efficiency was maximized. The large dependence of CAD and IRMPD on helium pressure is clear-cut, and the near 100% dissociation efficiency at the lower or optimal helium pressures rapidly falls to less than 10% as the helium pressure is raised. However, the trend for UVPD shows very little change as a function of helium pressure. This helium independence was also observed for other chromophore-derivatized peptides including ADSGEGDFLAEGGGVR, the largest peptide studied. We attribute the slight decrease in UVPD efficiency as the helium pressure increases to a small distortion in the size of the ion cloud, thus degrading its overlap with the UV laser beam profile. The lack of significant impact of the helium pressure on the UVPD efficiency is due to the fast time scale of energy deposition; the 10 ns period of the Q-switched laser pulse means that the internal energy deposition needed to promote ion dissociation occurs much faster than the time scale of collisional cooling. The energized precursor ions will either dissociate or cool in the period between laser pulses, but there is no evidence for accumulation of energy over several consecutive laser pulses.

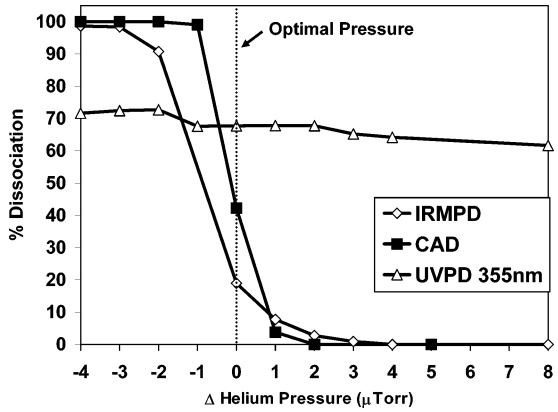


**Figure 9.** Percentage dissociation of the isolated precursor ion population (i.e., a measure of precursor ion disppearance) of (DNP)-PQG peptide versus relative helium pressure in the ion trap upon activation by IRMPD (20 W for 25 ms), CAD (0.49 V for 30 ms), or UVPD (355 nm, 2 pulses at 10 Hz). Normal optimal chamber pressure was measured as nominally ~30 $\mu$Torr (uncorrected), and variation from this optimal value is shown as a $\mu$Torr scale for the $x$-axis.

## CONCLUSION

UVPD at 355 nm of chromophore-derivatized peptides results in simple MS/MS spectra dominated by a clean series of y ions down to the $y_1$ ion, thus allowing facile sequencing of doubly protonated peptides through de novo interpretation. CAD and UVPD of AF350-derivatized singly protonated peptides also produce a clean series of y ions simplifying peptide sequence analysis. The success of this process for N-terminally modified peptides stems in part from the rapid secondary dissociation of chromophore-containing b ions, thus eliminating them from the spectra whereas the nonchromophore-containing y ions do not undergo further dissociation. C-Terminal lysine modification produced an array of a/b-type ions in the MS/MS spectra absent

of chromophore-containing y ions, further supporting this secondary dissociation mechanism. The pulsed nature of the Nd:YAG laser results in activation that is virtually independent of the helium pressure, which offers an extra degree of flexibility for MS/MS applications.

## ACKNOWLEDGMENT

Funding from the Welch Foundation (F1155), the National Science Foundation (CHE-0315337 and CHE-0718320) and an NSF/IGERT fellowship to J.J.W. (D6E-03333080) are gratefully acknowledged.

## SUPPORTING INFORMATION AVAILABLE

Additional information as noted in text including UVPD MS/MS spectra of singly and doubly protonated AMCA-FSWGAEGQR and DNP-FSWGAEGQR. This material is available free of charge via the Internet at http://pubs.acs.org.

Received for review June 12, 2007. Accepted August 1, 2007.

AC071241T